Supplemental Material

Jumping-Droplet Electrostatic Energy Harvesting

Nenad Miljkovic,[1] Daniel J. Preston,[1] Ryan Enright,[2] and Evelyn N. Wang[1,*]

[1]*Department of Mechanical Engineering, Massachusetts Institute of Technology, 77 Massachusetts Avenue, Cambridge, Massachusetts 02139, USA*
[2]*Thermal Management Research Group, Efficient Energy Transfer (ηET) Department, Bell Labs Ireland, Alcatel-Lucent Ireland Ltd., Blanchardstown Business & Technology Park, Snugborough Rd, Dublin 15, Ireland*

*Address correspondence to enwang@mit.edu

S.1 HIGH SPEED MOVIES

Movies 1, 2, and 3. Droplet jumping during condensation and electrostatic power generation between superhydrophobic CuO (dark vertical fins) and hydrophilic Cu fins (bright vertical fins) captured with a high speed camera (Phantom v7.1, Vision Research). The fins were aligned by interdigitating Cu heat sinks (combs) with dimensions 26 x 89 x 75 mm (height x width x depth) (E1U-NPFSS-30, Cooler Master). The fin surfaces were oriented vertically (gravity facing downwards). Many small droplets jumped laterally from the CuO surfaces and landed on the adjacent Cu surfaces. Some jumping droplets reversed direction after jumping due to vapor flow entrainment and electrostatic repulsion and travelled back towards the CuO surface.[1] Once the returning droplets returned to the surface, they a) coalesced with other droplets on the surface and underwent a second jump,[2,3] or b) adhered to the CuO surface and grew *via* condensation until coalescing with a neighboring droplet and jumping from the surface again.[2] The vapor pressure was ≈1.8 kPa. The video was captured at 1000 fps and is played back at 20 fps. The field of view is 12.8 mm x 9.6 mm. Movie 2 corresponds to the false-color time-lapse images shown in Fig. 2(c) of the manuscript.

S.2 CONDENSATION CHAMBER SETUP

The custom environmental chamber used for this work (Kurt J. Lesker) consists of a stainless steel frame with a door (sealed with a rubber gasket), two viewing windows, and apertures for various components. Resistive heater lines were wrapped around the exterior of the chamber

walls to prevent condensation at the inside walls and then insulated on the exterior walls. The output power of the resistive heater lines was controlled by a voltage regulator (Variac). Two insulated stainless steel water flow lines (Swagelok) were fed into the chamber *via* a KF flange port (Kurt J. Lesker) to supply cooling water to the chamber from a large capacity chiller (System III, Neslab). The cooling water flow rate was measured *via* an in-line liquid flow meter (0-5 L/min L-Series liquid flow meter, Alicat)

A secondary stainless steel tube line was fed into the chamber *via* a KF adapter port that served as the flow line for the incoming water vapor supplied from a heated steel water reservoir. The vapor line was wrapped with a rope heater (60 W, Omega) and controlled by a power supply (Agilent). The vapor reservoir was wrapped with another independently-controlled rope heater (120 W, Omega) and insulated to limit heat losses to the environment. The access tubes were welded to the vapor reservoir, each with independently-controlled valves. The first valve (Diaphragm Type, Swagelok), connecting the bottom of the reservoir to the ambient, was used to fill the reservoir with water. The second valve (BK-60, Swagelok), connecting the top of the reservoir to the inside of the chamber, provided a path for vapor inflow. K-type thermocouples were located along the length of the water vapor reservoir to monitor temperature.

A bellows valve (Kurt J. Lesker) was attached to the chamber to serve as a leak port between the ambient and inside of the chamber. In order to monitor temperatures within the chamber, K-type thermocouple bundles were connected through the chamber apertures *via* a thermocouple feed through (Kurt J. Lesker). To provide electrical connections inside the chamber for LED lighting and electric field generation, insulated copper electrical wires were connected through the chamber apertures *via* an electrical feed through (Kurt J. Lesker). A pressure transducer (925 Micro Pirani, MKS) was attached to monitor pressure within the chamber. The thermocouple bundles and the pressure transducer were both electrically connected to an analog input source (RAQ DAQ, National Instruments), which was interfaced to a computer for data recording. A second bellows valve (Kurt J. Lesker) was integrated onto the chamber for the vacuum pump, which brought down the chamber to vacuum conditions prior to vapor filling. A liquid nitrogen cold trap was incorporated along the line from the chamber to the vacuum which served to remove any moisture from the pump-down process and ultimately assist in

yielding higher quality vacuum conditions. A tertiary bellows valve (Kurt J. Lesker) was integrated on a T fitting between the vacuum pump and liquid nitrogen reservoir to connect the vacuum line to the ambient to release the vacuum line to ambient conditions once pump down was achieved. In order to visually record data, a high speed camera (Phantom v7.1, Vision Research) was placed in line with the 5" viewing windows on the chamber. The schematic of the exterior of the environmental setup is depicted in Fig. S1(a). Images of the front and rear of the experimental setup are shown in Fig. S1(b) and Fig. S1(c), respectively.

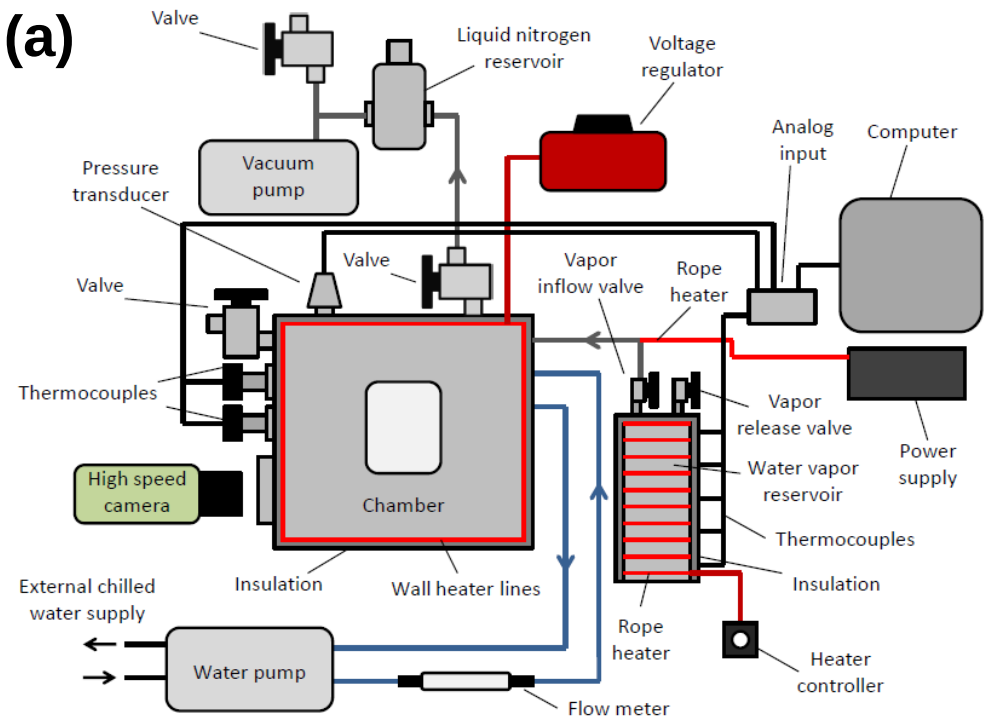

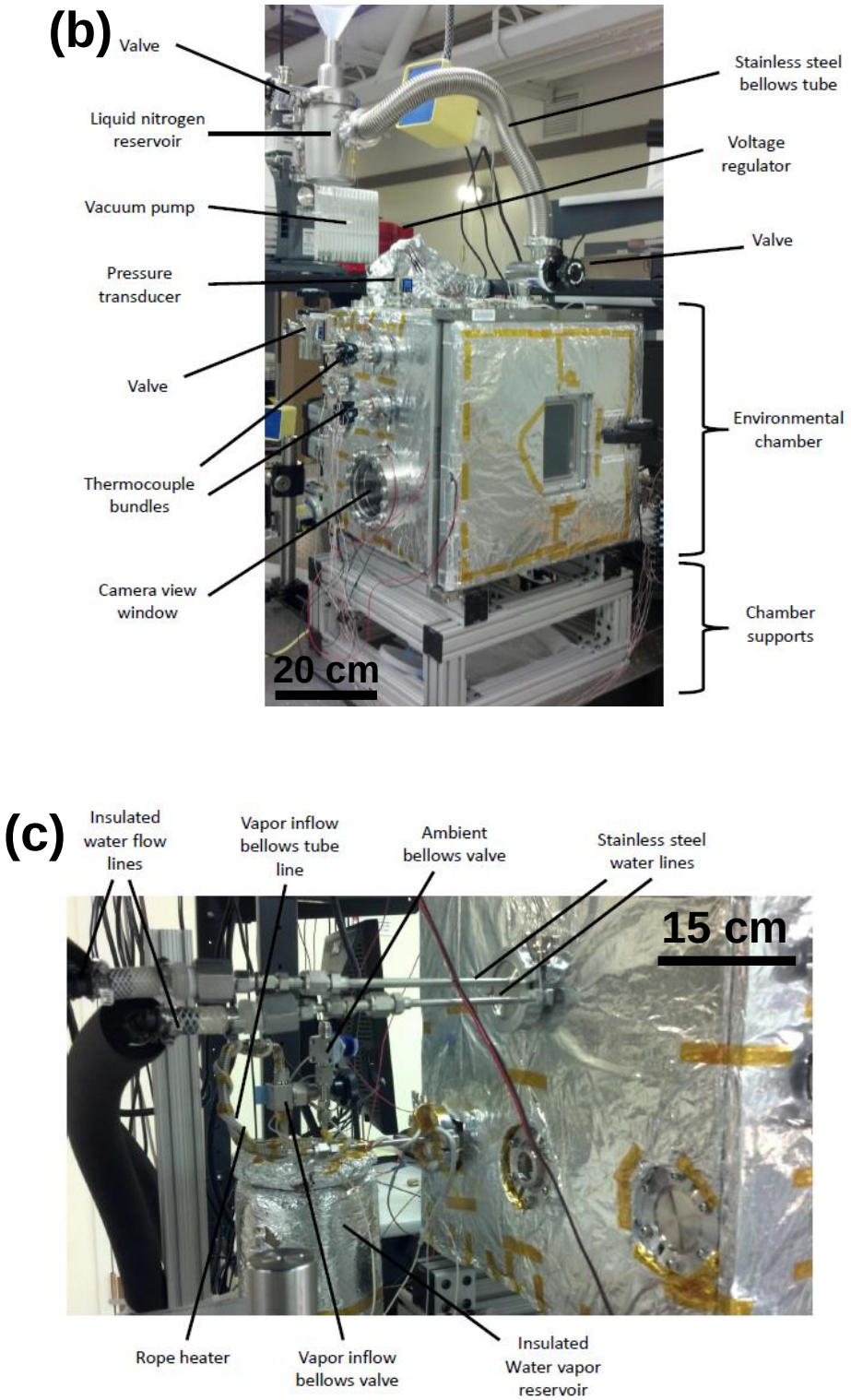

FIG. S1. (a) Schematic of experimental setup (not to scale). (b) Image of the experimental setup shown from the front (high speed camera and data acquisition system not shown). (c) Image of the experimental setup from the rear of the chamber showing the cooling water inlet and outlet and water vapor reservoir.[4] Reprinted with permission from Reference 4. Copyright 2012 American Chemical Society.

The setup used to run experiments inside the chamber is shown in Fig S2. Stainless steel bellows tube lines (1/4”, Swagelok) were connected to the external water flow lines (Fig. S1(c)). T-connection adapters (Swagelok) with bore through Ultra-Torr fittings (Swagelok) were used to adapt K-type thermocouple probes (Omega) at the water inlet and outlet.

The interdigitated comb test platform consisted of a 10.1 x 8.7 x 0.49 cm custom made copper cold plate which was connected *via* a Swagelok compression fitting onto the T-connection. The cold plate was manufactured by bending a heat treated a 1/4” Cu tube into and S-shape to increase contact area (Fig. S2(a)), milling a channel in the shape of the tube into a Cu block (Fig. S2(b)), and soldering the Cu tube to the channel (Fig. S2(c, d)). The back side of the cold plate remained flat in order to hold the interdigitated comb device (Fig. S2(e)). The cold plate tube was then connected *via* a Swagelok compression fitting onto the stainless steel cooling water flow bellows tube lines (Fig. S3). Chilled water flows through the inlet bellows tube, along the inside of the cold plate and through the outlet. One support was used to hold the cold plate and the entire configuration in place.

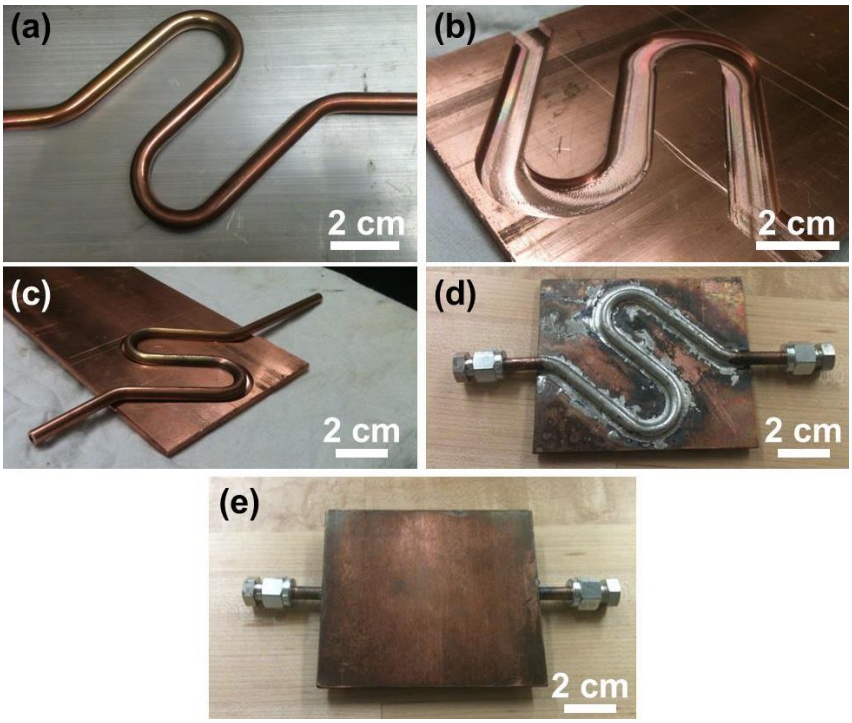

FIG. S2. Image of the cold-plate fabrication steps showing (a) 1/4" Cu heat treated tube after bending, (b) milled Cu cold plate block, (c) the tube resting in the milled cold plate block, (d) the cold plate after soldering, and (e) the cold plate front side (opposite of the soldering side).

S.3 CONDENSATION PROCEDURE

For each experimental run, a set of strict procedures were followed to ensure consistency throughout the experiments. The first step of the process was to turn on the voltage regulator to heat up the environmental chamber walls, which prevented condensation on the chamber walls. Simultaneously, the water vapor reservoir was filled with approximately 3.5 liters of DI water (99% full) using a syringe through the vapor release valve. After opening the vapor inflow valve and closing the vapor release valve, the rope heater around the water vapor reservoir was turned on with the heater controller set to maximum output (120 W). Then the rope heater connected to the vapor inflow valve was turned on. The temperature of the water reservoir was monitored with the installed thermocouples; the temperature at the top of the reservoir was higher than that of the middle/bottom of the reservoir due to the water thermal-mass present at the middle/bottom section. Hence, we ensured that the regions of the water reservoir of higher thermal capacity were brought to a sufficiently high temperature for boiling. During the boiling process, aluminum foil was placed on the bottom surface of the inner chamber to collect any of the water leaving the vapor inflow line. Once boiling was achieved and all thermocouples on the reservoir were >100˚C for at least 10 minutes, the vapor inflow valve was closed. The excess water that spilled inside the chamber during de-gassing of the reservoir was removed.

To install the cold plate onto the rig (Fig. S2), the Swagelok female adapters at the ends of the cold plate were connected to the 90 degree male elbow connecters on the rig. Before installing the cold plate in the chamber, all adapters/connecters were tightened to ensure that there were no leaks that could affect vacuum performance. The cold plate was then placed on top of the steel support and the bellows tubes (for the water inflow/outflow) were connected to the water lines (Fig. S3). After installation of the cold plate, the superhydrophobic CuO comb was placed on the cold plate surface with fins facing upwards and fin gaps aligned with the high speed camera viewport. To offset the hydrophilic Cu comb, four cylindrical Teflon spacers were placed at the four corners of the CuO comb (Fig. S3(b)). The Cu comb was placed on top of the spacers facing downward and aligning the fins to fit between the CuO fins and not make contact (interdigitating the two combs). The Teflon spacers not only electrically isolated the two combs, they acted as thermal insulation to ensure that only the CuO comb is cooled by the cold plate and avoid condensation on the Cu comb.

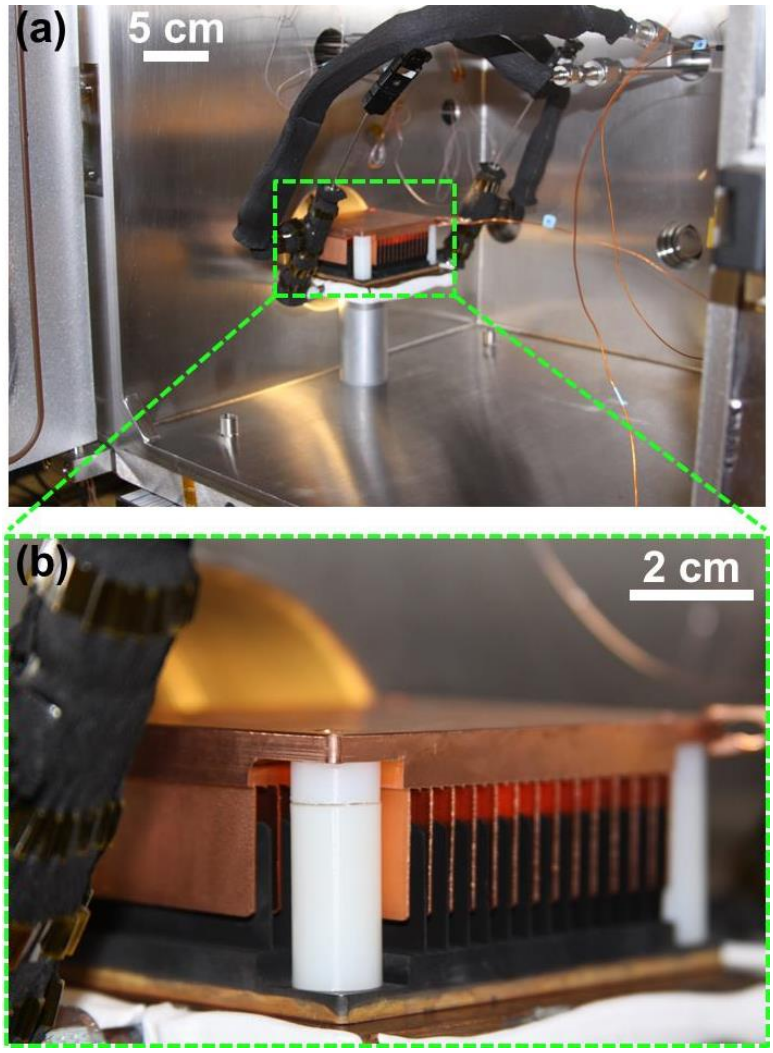

FIG. S3. (a) Image of the experimental setup inside the chamber with a (b) magnified view of the cold-plate showing the interdigitated CuO and Cu combs sitting on top. The base of the superhydrophobic CuO comb was in contact with the cold plate, while the hydrophilic Cu comb rested on top of the four Teflon spacers (white cylinders) and was electrically and thermally insulated from the CuO comb. To electrically insulate the CuO comb from the cold plate, Kapton tape was applied on top of the cold-plate surface.

Electrical Measurement Setup

To measure the electrostatic power potential of the interdigitated device, we measured the open circuit voltage (V_{OC}) and short circuit current (I_{CS}) during condensation. A high accuracy electrometer (6517B, Keithley Instruments) was electrically connected with a triaxial cable to the interdigitated combs *via* an electrical feed through (Kurt J. Lesker) mounted on a chamber aperture. Inside the chamber, the combs were connected to the electrical feed through *via*

insulated copper electrical wires. The electrometer was electrically connected (GPIB) to an analog input source (RAQ DAQ, National Instruments), which was interfaced to a computer for data recording.

Figures S4(a) and S4(b) show diagrams of the electrical connections used during the experiments to measure V_{OC} and I_{SC}, respectively. The chamber and electrometer chassis were grounded to the optical table. The chamber acted as both a ground and a shield for the electrical measurements.

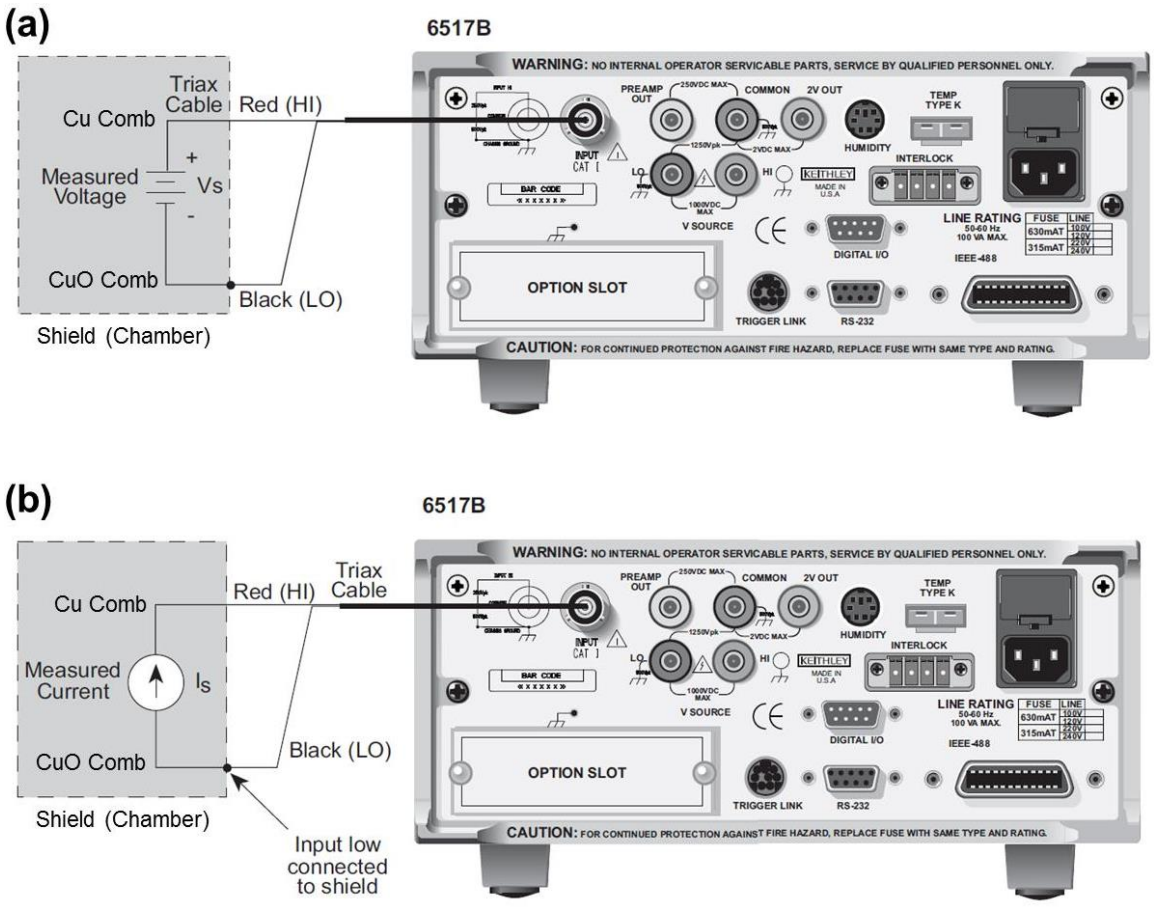

FIG. S4. Electrical circuit schematics of the (a) open circuit voltage, V_{OC} and (b) short circuit current, I_{SC}, measurement.[5] Copyright © Tektronix. All Rights Reserved. Reprinted with permission from Reference 5.

Condensation Procedure

Once the experimental setup was installed inside the chamber and the electrical connections (Fig. S4) were double checked for electrical shorts, the next step was to begin the vacuum pump-down procedure. Initially, the liquid nitrogen cold trap was filled to half capacity. The ambient exposed valves connecting the chamber and the vacuum pump were both closed and the valve connected to the liquid nitrogen cold trap was opened. The vacuum pump was then turned on, initiating the pump-down process. The pressure inside the chamber was monitored during the pump-down process. This process took approximately one hour in order to achieve the target vacuum conditions (0.5 Pa < P < 1 Pa). The experimental operating pressure of non-condensable was set to be a maximum of 0.25% of the operating pressure. In our experiments, extreme care was taken to properly de-gas the vacuum chamber and water vapor reservoir prior to experimental testing.

The setup of the water flow-loop is described as follows. The Neslab water pump reservoir was filled and turned on to a flow rate of 5 ± 0.25 L/min. The flow rate was monitored with the flow meter integrated in the inflow water line (0-5 L/min L-Series liquid flow meter, Alicat). In order to bring the chilled water into the flow loop and to the tube sample, the external chilled water lines were opened.

Prior to beginning the experiments, the high-speed camera was turned on for visual recording of the sample during condensation. Afterwards, the rope heater around the water reservoir was turned off and the vapor inflow valve was slowly turned open until the operating pressure was reached. Once the operating pressure was reached, the vapor inflow valve was closed and the vapor was allowed to reach thermal equilibrium inside the chamber. To initiate the condensation process for the short circuit measurement (Fig. S5), the chilled water supply temperature (T_c) was decreased (t ≈ 16 minutes) until jumping droplet condensation was observed between the fins of the interdigitated device (Movies 1-3). During condensation, the vapor pressure (P_v) decreased due to the finite amount of vapor inside the chamber and T_c was maintained at ≈7.1°C. As the condensation process intensified due to transient cooling of the CuO fins, I_{SC} increased and eventually reached a quasi-steady value of $I_{SC} \approx 1.1 \pm 0.05$ nA (t ≈ 17.5 minutes). After approximately 30 seconds of reaching a steady measurement, the cooling water temperature was increased (t ≈ 18 minutes) and I_{SC} slowly decayed with time due to the smaller supersaturation

for condensation, and lower droplet jumping frequency. At $t \approx 22$ minutes, the chamber was vented *via* the bellows vent valve and condensation abruptly ended, resulting in the short circuit current decreasing rapidly to zero.

Note, during the short circuit test, T_c was lower than the saturation temperature at the water vapor pressure ($T_{sat}(P_v)$) in the chamber prior to condensation initiating ($t < 16$ minutes). This was due to the fin conduction resistance and temperature drop from the fin surface to the cooling water. In actuality, the fins surface was above $T_{sat}(P_v)$ until the cooling water temperature was lowered below 8°C.

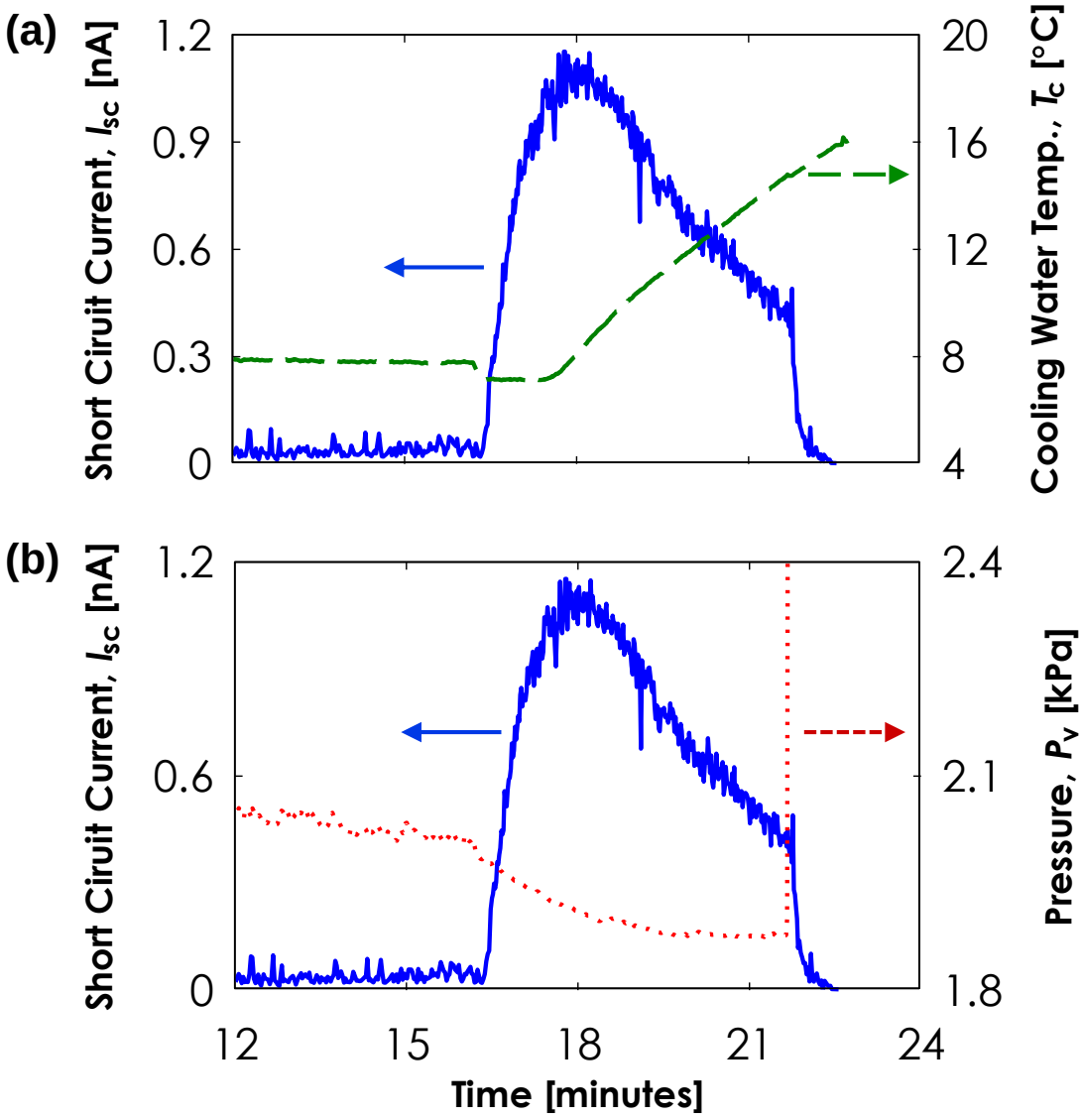

FIG. S5. Short circuit current (I_{SC}) measurement as a function of time (t) with (a) vapor pressure and (b) cooling water temperature overlaid.

References:

[1]N. Miljkovic, D. J. Preston, R. Enright, and E. N. Wang, ACS Nano **7** (12), 11043 (2013).
[2]N. Miljkovic, D. J. Preston, R. Enright, and E. N. Wang, arXiv:1310.2975 [physics.flu-dyn] (2013).
[3]K. Rykaczewski, A. T. Paxson, S. Anand, X. Chen, Z. Wang, and K. K. Varanasi, Langmuir **29** (3), 881 (2013).
[4]N. Miljkovic, R. Enright, Y. Nam, K. Lopez, N. Dou, J. Sack, and E. N. Wang, Nano Letters **13** (1), 179 (2013).
[5]Keithley Instruments, *Model 6517B Electrometer User's Manual*, 6517B-900-01 Rev. A / Jun 2008, 2008.